Chemical Physics Letters 637 (2015) 51–57

Contents lists available at ScienceDirect

Chemical Physics Letters

journal homepage: www.elsevier.com/locate/cplett

Approaching the double-faceted nature of the CX bond in halobenzenes with a bifunctional probe

Krystel El Hage[a,b,1], Jean-Philip Piquemal[c], Zeina Hobaika[b], Richard G. Maroun[b], Nohad Gresh[a,c,*]

[a] Chemistry and Biology Nucleo(s)tides and Immunology for Therapy (CBNIT), UMR 8601 CNRS, UFR Biomédicale, Paris, France
[b] Centre d'Analyses et de Recherche, UR EGFEM, LSIM, Faculté des Sciences, Saint Joseph University of Beirut, B.P. 11-514 Riad El Solh, Beirut 1107 2050, Lebanon
[c] Laboratoire de Chimie Théorique, Sorbonne Universités, UPMC, UMR7616 CNRS, Paris, France

ARTICLE INFO

Article history:
Received 4 May 2015
In final form 25 July 2015
Available online 7 August 2015

ABSTRACT

In halobenzenes, the CX bond (X = Cl, Br) is doubly faceted, electron-deficient along the CX direction, and electron-rich on its flanks. We have recently shown that both features could be enhanced by appropriate electron-withdrawing and electron-donating groups, respectively. In this letter we further highlight this dual character by approaching a bifunctional probe, N-methylformamide, to both regions in representative substituted halobenzenes. We report the results of interaction energy computations, ELF, and NCI analyses. These methods used in conjunction show the responsiveness of the CX bond to both kinds of substitutions, enabling significant interaction energy gains with respect to the parent compound.

1. Introduction

In Cl, Br, and I halobenzenes the zone of electron depletion which prolongs the C–X bond, the 'sigma hole', coexists with a zone of electron build-up on its sides [1–3]. Leveraging electron depletion is focusing much interest [4–11]. Thus several examples show the CX bond pointing directly toward an electron-rich atomic site, such as the main-chain carbonyl of proteins, or toward the center of the electron-rich aromatic rings. Examples are provided by protein [12–21] and DNA [22] recognition sites of halobenzenes, by molecular crystals [23,24] and by supramolecular chemistry [25]. Studies aiming to leverage the electron buildup, on the other hand, remain scarce. This was addressed in two recent studies from our laboratories [26,27]. Dispersion-corrected DFT computations enabled to compare the interaction energies of several substituted derivatives of the chlorobenzene ring of known drugs with target binding sites of three proteins. Along with the parent compound, we considered derivatives substituted with electron-withdrawing, electron-donating groups, or combinations of both. Electron-donating groups, and not only electron-withdrawing ones, were found in some cases to significantly increase the interaction energies with the targeted sites. This was due to the presence of an electron-deficient site close to the electron-rich cone of the CX bond. Furthermore, both electron-donating and electron-withdrawing groups could coexist within the same halobenzene derivative, leading to independent and in some cases possibly concerted, enhancements of ΔE.

In the present letter, we further elaborate on the dual character of chloro- and bromo-benzene and some of their derivatives. These are probed by an incoming ligand which is itself bifunctional, namely N-methylformamide (NMF). NMF is the building block of the protein backbone, and can act through its NH group as a proton donor to the electron-rich cone of the CX bond and/or to the electron-rich ring of the benzene ring, and, through its CO bond, as an 'X-bond acceptor' from the sigma-hole.

We compare the differences, $\delta\Delta E_{binding}$ between the values of the interaction energies ($\Delta E_{binding}$) in the different binding modes, as well as those with 'bare', unsubstituted benzene. Simultaneous binding of two NMF probes is subsequently investigated and energy-minimized, to assess the possibility of mutual coexistence of the two modes.

As a complement to the energy trends, we report analyses of the electron density redistribution occurring in the NMF complexes, using two procedures, the non-covalent interaction (NCI) and the electron localization function (ELF).

* Corresponding author at: Laboratoire de Chimie Théorique, Sorbonne Universités, UPMC, UMR7616 CNRS, Paris, France.
E-mail address: gresh@lct.jussieu.fr (N. Gresh).
[1] Current address: Department of Chemistry, University of Basel, Klingelbergstrasse 80, 4056 Basel, Switzerland.

http://dx.doi.org/10.1016/j.cplett.2015.07.047
0009-2614/

2. Procedure

The intermolecular interaction energies were computed at the correlated level, using the dispersion-corrected B97-D functional by Grimme [28]. Since as shown in our previous paper [27], other functionals, such as WB97X [29] and M062X [30] gave consistent results with B97-D, we resorted here solely to it. We used the aug-cc-pVTZ(-f) basis set [31,32]. Energy-minimization was done in the gas phase to account for the fact that the immediate environment of the complexes is shielded from water. This was done with the Berny procedure [33–40] coded in the G09 software [41]. The values of ΔE were corrected for BSSE [42,43]. The solvation energies of the uncomplexed halobenzenes were computed with the C-PCM procedure, a conductor-like polarizable continuum model [44,45]. The complex within the recognition site was not solvated, since it is buried in the protein binding site. The binding energy ΔE is expressed as:

$$\Delta E_{\text{binding}} = \Delta E_{\text{complex}} - (E_{\text{prot/DNA}} + E_{\text{lig}}) \quad (1)$$

It represents the difference between the energy of the complex and those of the individual interacting molecules. E_{lig} is the energy of the ligand optimized prior to interaction in a water continuum.

The energy balances are completed upon including the desolvation energy of the inhibitor, $\delta\Delta E_{\text{solv}}$ prior to binding, so that $\Delta E_{\text{fin}} = \Delta E_{\text{binding}} + \delta\Delta G_{\text{solv}}$. ΔE_{fin} is thus the final energy balance.

For representative complexes, analyses of the electron populations and volumes on the halogen atom were done using the ELF analysis [46–48].

Analyses of the electron density redistribution resulting from the intermolecular interactions were done using the non-covalent interaction (NCI) procedure with the NCI-Plot program [49,50]. The NCI procedure is based on the study of the reduced density gradient as a function of density. It enables to visualize the weak interaction zones between two molecules and gives access, in a qualitative way, to the magnitude of these interactions.

3. Results and discussion

3.1. Intermolecular interactions

The energy-minimized positions of approach of NMF to benzene, chloro- and bromobenzene are represented in Figures 1 and 2, regarding the through-CO and through-NH approaches, respectively. The optimized intermolecular variables of approach are also represented in these figures.

3.1.1. Binding to the electron-deficient (α^+) zone

The energy-minimized position of approach of the carbonyl O atom to benzene locates the CO bond midway between two CH bonds. Those for CO binding to chloro- and bromobenzene are along the CCl and CBr bonds, the NMF plane being perpendicular to halobenzene. Consistent with the results by Hobza and coworkers [5], bromobenzene has a more favorable ΔE with NMF than chlorobenzene (−2.4 kcal/mol versus −1.6 kcal/mol, respectively), on account of the greater electron depletion along the C–Br bond. The Br–O distance is shorter than the Cl–O one (3.2 Å versus 3.3 Å, respectively) even though Br is bulkier than Cl. Through-CO NMF binding to unsubstituted benzene is nevertheless 0.7 kcal/mol more favorable than to bromobenzene. Such unconstrained complexes could represent, however, idealized situations, because in practical situations, both interacting entities could have restricted accessibilities and mobilities due to their anchoring in larger molecules.

3.1.2. Binding to the electron-rich (α^-) zone

The optimized binding position of NMF to unsubstituted benzene has the NH bond virtually perpendicular to the electron-rich benzene ring, and shifted toward its center. In its binding to chloro- and bromobenzene, the NH bond is inclined with respect to the ring, so that the NH proton locates in the electron-rich cone. This also enables the formamide moiety to partially stack over the benzene ring and the acidic proton of the CH bond to lie over the center of the ring. Partial stacking of the protein backbone and the halobenzene ring of an inhibitor was observed in the X-ray crystal structure of human cathepsin with synthetic inhibitors [12]. ΔE is, again, more favorable for bromo- than chlorobenzene (−5.7 kcal/mol versus −5.2 kcal/mol), and less favorable than for benzene binding by a reduced difference (0.4 kcal/mol) compared to the situation with the CO approach.

Thus in the model NMF complexes, the NH approach to the α^- site of the CX bond appears more than twice as favorable than the CO approach to the α^+ region, yet it is the latter mode of binding that is the most frequently sought after for the design of halobenzene derivatives with enhanced binding properties.

The simultaneous interaction of two NMF probes was subsequently energy-minimized showing both coexisting in the ternary complex without significantly perturbing their positions in the binary complexes.

The distinctive features of the α^- and α^+ regions can be amplified by (a) electron-withdrawing and (b) electron-donating substituents. We have thus considered the following substitutions: for (a) monosubstitution by NO_2 in para, thus electron-withdrawal by mesomeric effects; disubstitution by F in meta, thus electron-withdrawal by inductive effects; and trisubstitution by both meta-F and para-NO_2; for (b) monosubstitution by –OH and –NH_2, thus electron-donation.

The ΔE values are reported in Table 1. In the binary complexes, and for the through-CO approach, while the OH and NH_2 electron-donors exert a weak destabilization, the NO_2 and F electron-attractors exert a clear enhancement of the binding. It ranges from −0.6 in para-fluorobenzene to −1.4 kcal/mol in para-nitro, dimeta-fluoro-bromobenzene. The CBr bond is more responsive than the CCl bond. For the through-NH approach, monosubstitution enhances the interaction energies by amounts in the range −1.3 kcal/mol (para-hydroxy-chlorobenzene) to −2.24 kcal/mol (para-amino-chlorobenzene). Regarding the electron attractors, monosubstitution by nitro in para and disubstitution by fluorine in meta are seen to destabilize binding by limited amounts, 0.1–0.3 kcal/mol, while surprisingly trisubstitution enhances it by −0.4 kcal/mol.

The values of ΔE in the ternary complexes have slightly (app. 0.20 kcal/mol) diminished magnitudes as compared to their corresponding sums in the two binary complexes. This is due to the small rearrangements occurring following the approach of the second NMF, and also to some non-additivity which was previously analyzed by parallel DFT-D and polarizable molecular mechanics studies [34]. Overall, the three most stable complexes are the ones with one electron-donor substituent, namely para-amino chlorobenzene and para-amino-bromobenzene and one with three electron-withdrawing substituents, namely two fluorines in meta and one nitro in para.

We have also monitored the evolutions of the interaction energies of bromobenzene, para-amino-bromobenzene and meta-difluoro-bromobenzene in their ternary complexes with two NMF ligands as a function of the N–Br distance of approach (Figure 3). Upon increasing the distance by up to 0.3 Å, ΔE undergoes shallow decreases in magnitude with all three bromobenzenes. The corresponding decreases in magnitude are steeper upon decreasing the distances, owing to the increased short-range Pauli repulsions. These decreases are the steepest, in fact, with the unsubstituted bromobenzene. Since with electron-withdrawing substituents, such as the two meta-fluorine atoms, the Pauli repulsion between Br and NMF is smaller, a lessened magnitude

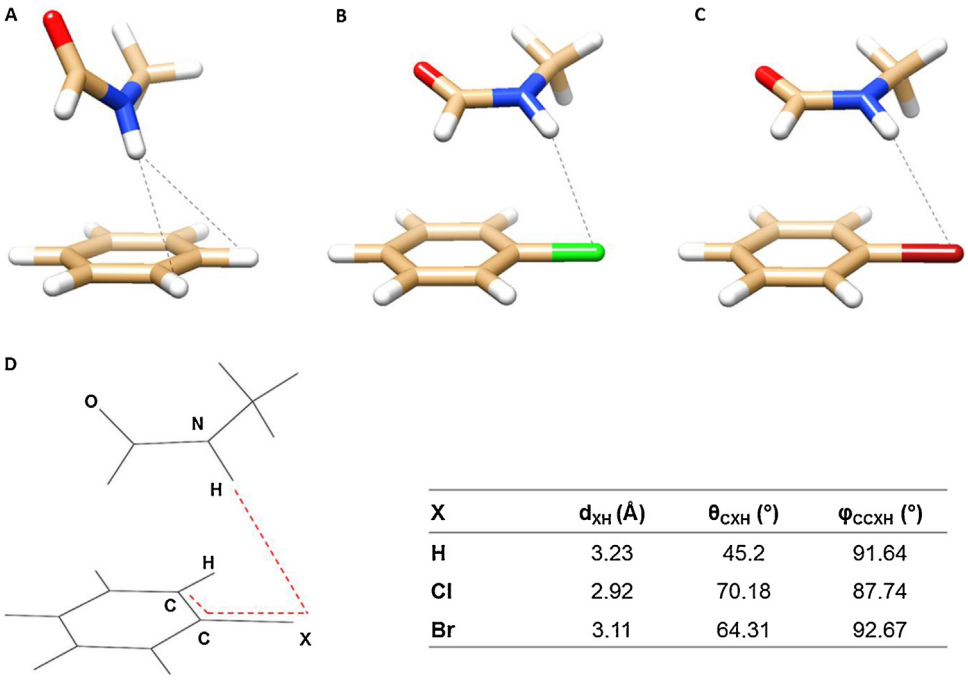

X	d_{XH} (Å)	θ_{CXH} (°)	φ_{CCXH} (°)
H	3.23	45.2	91.64
Cl	2.92	70.18	87.74
Br	3.11	64.31	92.67

Figure 1. Optimized position of the binary complexes for the NH approach. (A) Optimized position for X = H, (B) optimized position for X = Cl and (C) optimized position for X = Br. (D) Optimized parameters (distance r, angle θ and angle φ).

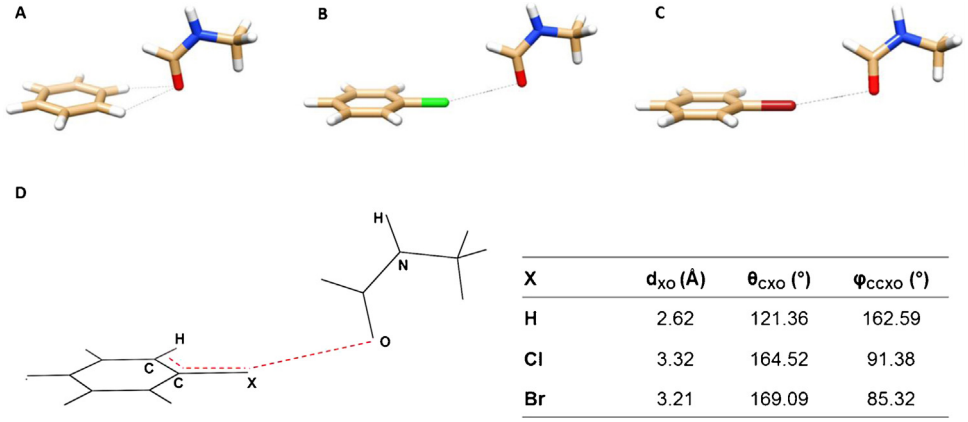

X	d_{XO} (Å)	θ_{CXO} (°)	φ_{CCXO} (°)
H	2.62	121.36	162.59
Cl	3.32	164.52	91.38
Br	3.21	169.09	85.32

Figure 2. Optimized position of the binary complexes for the O approach. (A) Optimized position for X = H, (B) optimized position for X = Cl and (C) optimized position for X = Br. (D) Optimized parameters (distance r, angle θ and angle φ).

Table 1
(A) Values of the interaction energies (kcal/mol) of NMF to benzene, chloro- and bromobenzene, with the corresponding unsubstituted ring as energy zero in gas phase. (B) Solvation energy of each ligand. (C) Values of the interaction energies of the ternary complex in solution phase.

A	Substitution	ΔE_{gas}, kcal/mol								
		O-approach			N-approach			Ternary complex		
		H	Cl	Br	H	Cl	Br	H	Cl	Br
	OH	−0.23	0.11 $\downarrow\alpha^+$	0.10 $\downarrow\alpha^+$	−1.01	−1.64 $\uparrow\alpha^-$	−1.33 $\uparrow\alpha^-$	−1.43	−1.30	−1.10
	NH_2	0.12	0.30 $\downarrow\alpha^+$	0.38 $\downarrow\alpha^+$	−1.83	−2.24 $\uparrow\alpha^-$	−2.11 $\uparrow\alpha^-$	−1.81	−1.68	−1.61
	NO_2	−1.10	−0.67 $\uparrow\alpha^+$	−0.88 $\uparrow\alpha^+$	1.16	0.20 $\downarrow\alpha^-$	0.32 $\downarrow\alpha^-$	−0.10	−0.44	−0.53
	2F	−0.82	−0.39 $\uparrow\alpha^+$	−0.55 $\uparrow\alpha^+$	1.00	0.00 $\downarrow\alpha^-$	0.07 $\downarrow\alpha^-$	−0.18	−0.41	−0.54
	2F-NO_2	−1.73	−1.09 $\uparrow\alpha^+$	−1.43 $\uparrow\alpha^+$	1.34	−0.10 $\downarrow\alpha^-$	−0.41 $\downarrow\alpha^-$	−0.68	−0.88	−1.71

B	Ligands	$\delta\Delta E_{Solv}$, kcal/mol		
	Substitution	H	Cl	Br
	OH	−7.03	−7.3	−7.26
	NH_2	−4.89	−5.55	−5.51
	NO_2	−5.31	−4.24	−4.24
	2F	−0.67	0.64	0.62
	2F-NO_2	−8.02	−5.78	−5.79

C	Ternary complex	$\Delta E_{gas} - \delta\Delta E_{Solv}$, kcal/mol		
	Substitution	H	Cl	Br
	OH	5.60	6.00	6.16
	NH_2	3.08	3.87	3.90
	NO_2	5.21	3.80	3.71
	2F	0.49	−1.05	−1.16
	2F-NO_2	7.34	4.90	4.08

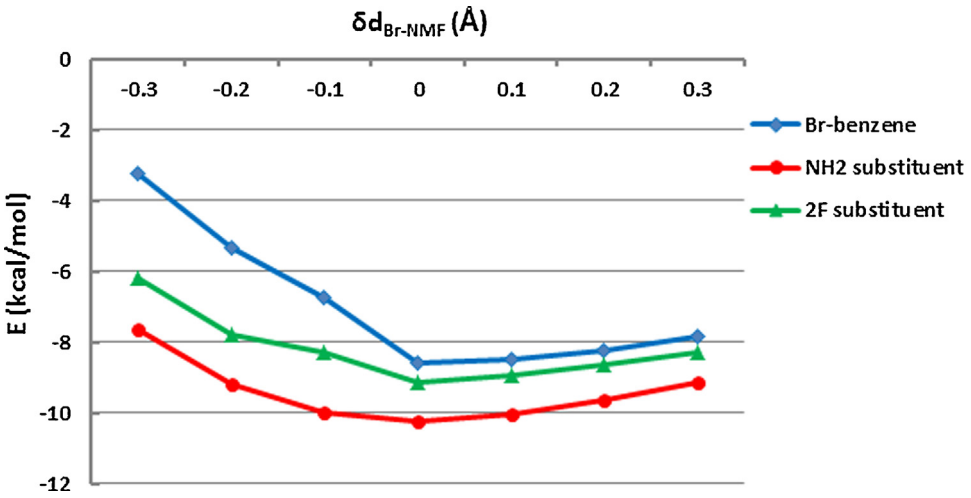

Figure 3. Variations of the intermolecular interaction energies (in kcal/mol) of bromobenzene, para-amino-bromobenzene and meta-difluoro-bromobenzene in their ternary complexes with two NMF ligands. δd_{Br-NMF} (in Angstrom units) denotes the distance increment/decrement with respect to equilibrium distance.

decrease upon distance reduction is expectable. The outcome with electron-donating substituent is less clear. The enrichment of the electron-rich cone around Br, resulting into an enhanced attraction for the electron-deficient sites of NMF, could partly overcome the increased Pauli repulsion, whence a less steep curve upon distance reduction than with the unsubstituted benzene.

For completeness, we have also included the calculation of the solvation energies of the individual ligands prior to complexation. Because of their polar natures, all substituents are seen to give rise to significantly larger solvation energies than the unsubstituted benzene or halobenzenes, with the exception of meta-difluoro-chloro- and bromobenzene. As a consequence, the resulting energy balances are unfavorable (Table 1C), except in the case of the ternary complexes of meta-difluoro-chloro- and -bromobenzene. This could possibly constitute an extreme case. On the one hand, the halobenzene when integrated into a 'complete' inhibitor could be much less accessible to solvation compared to its 'bare' model. On the other hand, the actual potential and field exerted by the protein recognition site on the halobenzene could further increase ΔE with respect to the model NMF complexes, particularly given the high polarizabilities of halobenzenes and their derivatives [26,27].

3.2. MEP and ELF analyses

We have also explored the electronic effects of substituents on the sigma hole, upon calculating the contours of the molecular electrostatic potential ('molecular electrostatic potentials', MEP) cores. These are commented in Supporting Information SI.1.

The MEP features are complemented by topological analyses, such as the electron localization function (ELF) [46–48]. Table 2 reports the results of ELF analyses of the volume and the electronic population V(Cl) around chlorine in chlorobenzene and its substituted derivatives. The volumes around Cl and C4-Cl are marked with arrows. With respect to unsubstituted chlorobenzene, comparison of these values gives quantitative values for the increases or decreases of both quantities upon substitution. We can observe that reductions of the volumes occur in the two binary complexes with one NMF, which is further accented in the ternary complex. The ranking of the derivatives in terms of volumes is the same in the complexed derivatives as in the uncomplexed ones.

For the representative ternary complex of bromobenzene with two NMF ligands, we have also monitored the evolutions of the electronic population and the volume, V(Br), around bromine as a function of increments/decrements, δd_{Br-NMF}, of the equilibrium distance separating Br from each NMF. These are reported in Supporting Information SI.3. Upon increasing the distance, V(Br) increases as a consequence of the reduced Pauli repulsions with the ligands. Conversely it decreases upon reducing the distance of approach, due to the increased Pauli repulsions. The electronic populations follow the same trends as the volumes, such that the ratio of the population over the volume remains constant (0.025) over distances spanning ±0.3 Å.

3.3. Non-covalent interaction (NCI) analysis

Using NCI [49,50], we have visualized the impact of substitutions on the redistribution of electron densities which take place in the ternary complexes with two NMF probes. Figure 4A–G illustrates the results for the ternary complexes of benzene, chlorobenzene, and its hydroxy-, amino-, difluoro, nitro, and difluoro-nitro-derivatives (see Supporting Information SI.2 for enlarged images).

Table 2
ELF analysis results of the electronic population and its volume V(Cl) around the chlorine atom in the most significant substituted derivatives. Population is given in e−, and the volume in au^3.

	No substitution	OH	NH_2	2F	NO_2	2F-NO_2
Volume V(Cl) au^3						
Uncomplexed	231.69	244.6	246.38	227.51	226.67	229.44
Ternary complex	195.85	207.02	208.26	192.34	191.04	193.02
NH-approach	210.49			208.22	208.14	208.77
OH-approach	228.74	238.92	240.18			
Population V(Cl) e−						
Uncomplexed	13.42	15.76	16.36	12.45	7.56	6.81

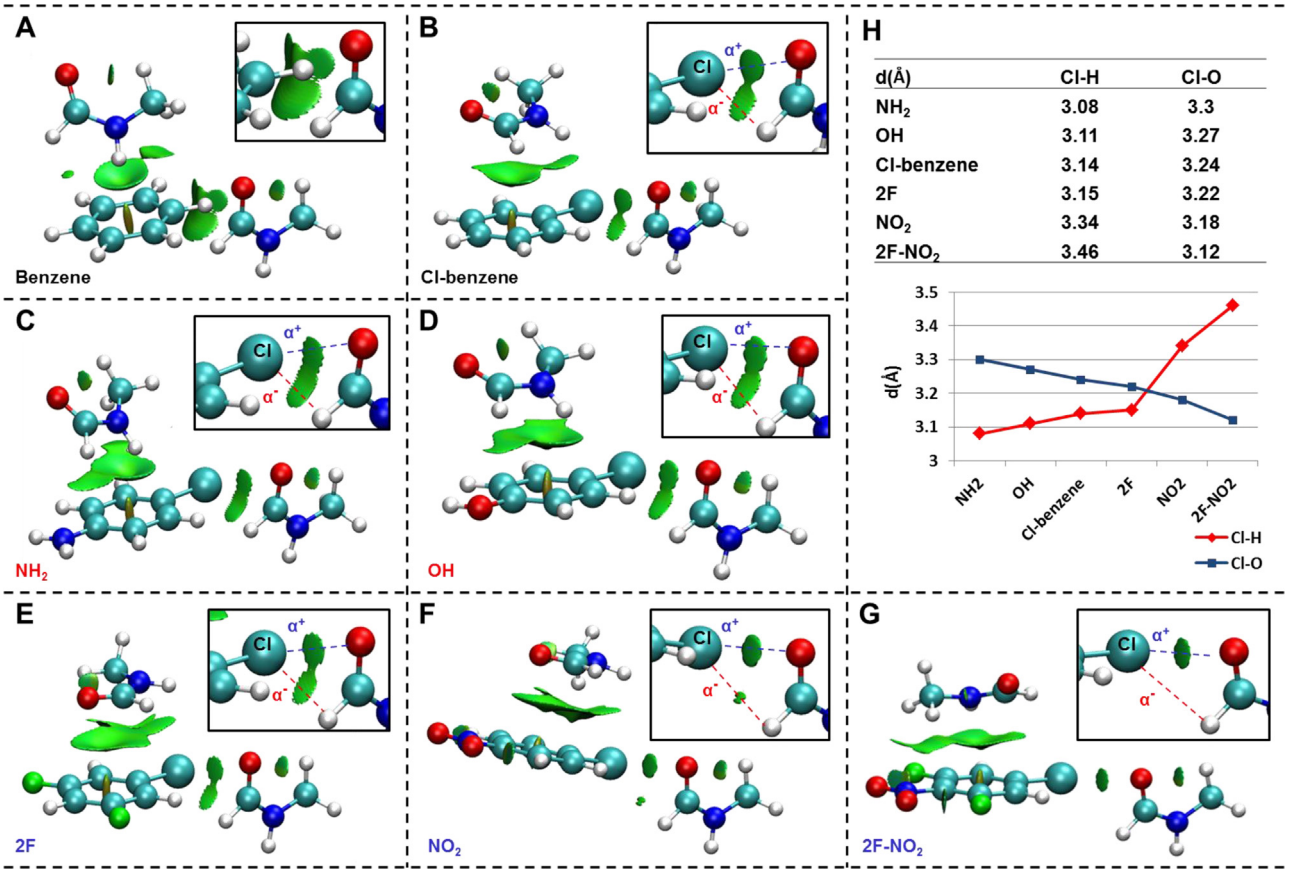

Figure 4. NCI plots of the halobenzene substituted models with the NMF probe, with a close-up on the double interaction of the CCl bond with the probe, in each case. The weak interactions are plotted with a green smear, the red dashed line represents the electron-rich region α^- and the blue dashed line represents the electron-deficient region α^+. (A) Benzene–NMF interaction; (B) Chlorobenzene–NMF interaction; (C) NH_2 substituent–NMF interaction; (D) OH substituent–NMF interaction; (e) 2F substituent–NMF interaction; (F) NO_2 substituent–NMF interaction; (G) 2F-NO_2 substituent–NMF interaction; (H) table and its corresponding plot of the variation of the equilibrium distance (in Å) between Cl and the amide H and with the carbonyl O as function of the substituent. (For interpretation of the references to color in this figure legend, the reader is referred to the web version of this article.)

The double-faceted interactions of the CCl bond is illustrated by the coexistence of two distinct surfaces between it and the through-CO approaching NMF (Figure 4B–G), indicative of stabilizing interactions. The α^+ zone interacts with the carbonyl O, and the α^- zone interacts with the acidic C-bound hydrogen. The present study is essentially exploratory, as there could be no CH interactions contributed by a protein, except those contributed by aromatic side-chains. It shows nevertheless that the α^- zone is wide enough to be accessible to main-chain or side-chain proton donor groups instead of the CH group, and that this could also occur in concert with the interaction with the sigma hole. With respect to unsubstituted chlorobenzene (Figure 4B), with para-hydroxy- and para-amino-chlorobenzene, a small build-up of the plot can be observed on the flanks of the α^- region together with a depletion of the α^+ region prolonging the CCl bond (Figure 4C and D). Thus enhanced binding to the NH group and weakened binding to the CO group are anticipated. The amino substituent is more effective in this respect than the hydroxy one, consistent with the more favorable ΔE values with para-amino- than para-hydroxychlorobenzene. Conversely, with electron-withdrawing substituents, electron depletion is observed on the flanks of the CCl bond along with a build-up of the plot prolonging it: this now translates enhanced binding to the CO group and weakened binding to the NH group. There is a progressive reduction of the α^- surface along the difluoro-, nitro-, and difluoro-nitro-chlorobenzene series (Figure 4E–G), the surface actually disappearing in the latter complex (Figure 4G). Such reductions are consistent as well with the evolutions of ΔE in this series. We have monitored in Figure 4H the evolution of the distance between Cl and the carbonyl O and the CH hydrogen. Consistent with the trends in ΔE and the two surfaces, we observe that the Cl–O distance decreases by up to 0.2 Å upon decreasing the electron-donating character or upon increasing the electron-withdrawing character of the substituent. Much more accented concomitant increases of the Cl–H distances take place in parallel, of up to 0.4 Å, upon passing from para-amino-chlorobenzene to difluoronitro-benzene. This attests to the attractive character of the electron-rich cone of chlorobenzene and its sensitivity to substitution.

An unanticipated feature of complexes A–G relates to the evolution of the orientation of the through-NH bound NMF with respect to the arene ring. It is perpendicular to it upon binding to unsubstituted benzene, so that the NH group interacts with the center of the electron-rich ring. It is inclined upon passing to chlorobenzene, so that the amide group could bind to the electron-rich cone of the C–Cl bond instead, while it is the acidic H of the CH group that now interacts with the arene ring center. It remains inclined following substitution with the two electron-rich donors, albeit the amide group is slightly shifted toward the center of the ring. Substitution with electron-withdrawing groups results into the NMF plane now virtually parallel to the halobenzene ring. Impoverishing the density on the latter favors its electrostatic interactions with the NMF π electron cloud. The nature of the interactions would evolve from hydrogen-bond-like with unsubstituted benzene to π–π in halobenzene derivatives substituted with electron-withdrawing

groups. With all three electron-withdrawing groups (Figure 4G), the overlap appears maximized.

4. Conclusions and perspectives

The present results lend further support to leveraging the electron-rich cone of the CCl and CBr bonds in halobenzenes as a means to enhance binding affinity. This was recently put forth in the case of three ligand–protein binding sites [26]. Such sites are however partly constrained owing to their anchoring in the macromolecule, preventing full optimization. In the present study we resorted to a bifunctional probe, NMF, to approach either the electron-rich cone of the CX bond by the NH and the partly acidic CH protons, or the sigma-hole by the CO bond. Using dispersion-corrected DFT, we fully optimized the binding of the probes to the two parent halobenzenes and to five of their substituted derivatives. This allows to fully unravel the binding potential of this cone. We found that through-NH NMF binding to it could with appropriate substituents give rise to even more favorable interaction energies than through-CO approach to the sigma hole. Bromobenzene was more responsive to electron-donating substituents than chlorobenzene, in line with experimental results [12]. NCI analyses on benzene, chlorobenzene and its derivatives complemented the inferences from the ΔE calculations. In chlorobenzene, they showed the appearance of an attractive surface between the electron-rich cone (denoted as α^-) and the approaching acidic C-bound hydrogen atom, and of a second one between the cone and the NH group of the second NMF approaching over the plane. The extent of the first surface increased upon increasing the electron-donor property of the para-substituent, from hydroxy to amino. It was reduced with electron-withdrawing substituents along the series bismetafluorine < para-nitro < bismeta-fluorine-para-nitro-chlorobenzene, actually vanishing with the latter. These trends paralleled the inverse trends of the Cl–H(C) distances. All these findings provide consistent evidence for the binding-prone character of the electron-rich cone, and its responsiveness to substitutions on the ring. It could be readily noted that in the absence of acidic CH hydrogens, the cone could be approached by a polar, N- or O-connected hydrogen without interference from an electron-rich atom independently approaching the sigma-hole. In fact, the cone could be enlarged, not only by electron-donating substituents, but also possibly by electron redistribution/polarization effects due to the approach of a second ligand on the other side of the ring.

In addition, from a structural standpoint, we observed a progressive alignment of the plane of the second NMF upon substitution. In benzene it was located perpendicular to the ring enabling the amide hydrogen to bind to the center. In chlorobenzene, a significant alignment occurred, enabling this hydrogen to preferentially interact over the Cl atom, with its electron-rich cone, leaving the less acidic CH hydrogen to bind to the ring center instead. With electron-withdrawing substituents, on the other hand, this NMF went parallel to the ring, a maximum overlap taking place with the three-substituted derivative. Such findings indicate that it could be possible to modulate the extent of overlap and mutual orientations of the ring and the conjugated molecule by appropriate substituents.

The present work is an added evidence in favor of the α^- cone, indicating new avenues to enhance, with appropriately selected electron-donor groups, the binding affinities of halobenzenes to their target sites.

Acknowledgments

We sincerely thank the Association Philippe Jabre for funding the PhD research of Krystel El Hage. We wish to thank the Grand Equipement National de Calcul Intensif (GENCI): Institut du Développement et des Ressources en Informatique Scientifique (IDRIS), Centre Informatique de l'Enseignement Supérieur (CINES), France, project No. x2009-075009), and the Centre de Ressources Informatiques de Haute Normandie (CRIHAN, Rouen, France), project 1998053. The authors also acknowledge the Research Council of Saint Joseph University of Beirut, Beirut, Lebanon (Project FS39), for financial support.

Appendix A. Supplementary data

Supplementary data associated with this article can be found, in the online version, at doi:10.1016/j.cplett.2015.07.047

References

[1] T. Clark, M. Hennemann, J.S. Murray, P. Politzer, J. Mol. Model. 13 (2007) 291.
[2] J.S. Murray, P. Lane, P. Politzer, J. Mol. Model. 15 (2009) 723.
[3] P. Politzer, J.S. Murray, T. Clark, Phys. Chem. Chem. Phys. 12 (2010) 7748.
[4] K.E. Riley, P. Hobza, J. Chem. Theory Comput. 4 (2008) 232.
[5] K.E. Riley, J.S. Murray, P. Politzer, M.C. Concha, P. Hobza, J. Chem. Theory Comput. 5 (2009) 155.
[6] M.A. Ibrahim, J. Comput. Chem. 32 (2011) 2564.
[7] W.L. Jorgensen, P. Schyman, J. Chem. Theory Comput. 8 (2012) 3895.
[8] R. Wilcken, M.O. Zimmermann, A. Lange, A.C. Joerger, F.M. Boeckler, J. Med. Chem. 56 (2013) 1363.
[9] T. Bereau, C. Kramer, M. Meuwly, J. Chem. Theory Comput. 9 (2013) 5450.
[10] K.E. Riley, J.S. Murray, J. Fanfrlik, J. Rezac, R.J. Sola, M.C. Concha, F.M. Ramos, P. Politzer, J. Mol. Model. 19 (2013) 4651.
[11] S. Jakobsen, T. Bereau, M. Meuwly, J. Phys. Chem. B 119 (2015) 3034.
[12] L.A. Hardegger, B. Kuhn, B. Spinnler, L. Anselm, R. Ecabert, M. Stihle, B. Gsell, R. Thoma, J. Diez, J. Benz, J.-M. Plancher, G. Hartmann, D.W. Banner, W. Haap, F. Diederich, Angew. Chem. Int. Ed. 50 (2011) 314.
[13] Y.X. Lu, T. Shi, Y. Wang, H. Yang, X. Yan, X. Luo, H. Jiang, W. Zhu, J. Med. Chem. 52 (2009) 2854.
[14] R. Battistutta, Cell. Mol. Life Sci. 66 (2009) 1868.
[15] L.J. Liu, W.A. Baase, B.W. Matthews, J. Mol. Biol. 385 (2009) 595.
[16] H. Matter, M. Nazare, S. Gussregen, D.W. Will, H. Schreuder, A. Bauer, M. Urmann, K. Ritter, M. Wagner, V. Wehner, Angew. Chem. Int. Ed. 48 (2009) 2911.
[17] N.F. Valadares, L.B. Salum, I. Polikarpov, A.D. Andricopulo, R.C. Garratt, J. Chem. Inf. Model. 49 (2009) 2606.
[18] E. Parisini, P. Metrangolo, T. Pilati, G. Resnati, G. Terraneo, Chem. Soc. Rev. 40 (2011) 2267.
[19] A.R. Voth, P.S. Ho, Curr. Top. Med. Chem. 7 (2007) 1336.
[20] A.R. Voth, P. Khuu, K. Oishi, P.S. Ho, Nat. Chem. 1 (2009) 74.
[21] R. Wilcken, X. Liu, M.O. Zimmermann, T.-J. Rutherford, A. Fersht, A. Joerger, A.F. Boeckler, J. Am. Chem. Soc. 134 (2012) 6810.
[22] P. Auffinger, F.A. Hay, E. Westhof, P.S. Ho, Proc. Natl. Acad. Sci. U. S. A. 101 (2004) 16789.
[23] J.P.M. Lommerse, A.J. Stone, R. Taylor, F.H. Allen, J. Am. Chem. Soc. 118 (1996) 3108.
[24] K.E. Riley, P. Hobza, Cryst. Growth Des. 11 (2011) 4272.
[25] A. Priimagi, G. Cavallo, P. Metrangolo, G. Resnati, Acc. Chem. Res. 46 (2013) 2686.
[26] K. El Hage, J.-P. Piquemal, Z. Hobaika, R.G. Maroun, N. Gresh, J. Comput. Chem. 36 (2015) 210.
[27] K. El Hage, J.-P. Piquemal, Z. Hobaika, R.G. Maroun, N. Gresh, J. Phys. Chem. A 118 (2014) 9772.
[28] S. Grimme, J. Comput. Chem. 27 (2006) 1787.
[29] J.D. Chai, M. Head-Gordon, J. Chem. Phys. 131 (2009) 174105.
[30] Y. Zhao, D.G. Truhlar, Theor. Chem. Acc. 120 (2008) 21.
[31] T.H. Dunning, J. Chem. Phys. 90 (1989) 1007.
[32] D. Feller, J. Comput. Chem. 17 (1996) 1571.
[33] H.B. Schlegel, Theor. Chem. Acc. 66 (2003) 333.
[34] R. Fletcher, Practical Methods of Optimization, Wiley, New York, 1980.
[35] J.M. Bofill, J. Comput. Chem. 15 (1994) 1.
[36] J.M. Bofill, N. Comajuan, J. Comput. Chem. 16 (1995) 1326.
[37] J. Simons, P. Jorgensen, H. Taylor, J. Ozment, J. Phys. Chem. 87 (1983) 2745.
[38] A. Banerjee, N. Adams, J. Simons, R. Shepard, J. Phys. Chem. 89 (1985) 52.
[39] J. Baker, J. Comput. Chem. 7 (1986) 385.
[40] J.T. Golab, D.L. Yeager, P. Jorgensen, Chem. Phys. 78 (1983) 175.
[41] M.J. Frisch, G.W. Trucks, H.B. Schlegel, G.E. Scuseria, M.A. Robb, J.R. Cheeseman, G. Scalmani, V. Barone, B. Mennucci, G.A. Petersson, H. Nakatsuji, M. Caricato, X. Li, H.P. Hratchian, A.F. Izmaylov, J. Bloino, G. Zheng, J.L. Sonnenberg, M. Hada, M. Ehara, K. Toyota, R. Fukuda, J. Hasegawa, M. Ishida, T. Nakajima, Y. Honda, O. Kitao, H. Nakai, T. Vreven, J.A. Montgomery Jr., J.E. Peralta, F. Ogliaro, M. Bearpark, J.J. Heyd, E. Brothers, K.N. Kudin, V.N. Staroverov, R. Kobayashi, J. Normand, K. Raghavachari, A. Rendell, J.C. Burant, S.S. Iyengar, J. Tomasi, M. Cossi, N. Rega, J.M. Millam, M. Klene, J.E. Knox, J.B. Cross, V. Bakken, C. Adamo, J. Jaramillo, R. Gomperts, R.E. Stratmann, O. Yazyev, A.J. Austin, R. Cammi, C. Pomelli, J.W.

Ochterski, R.L. Martin, K. Morokuma, V.G. Zakrzewski, G.A. Voth, P. Salvador, J.J. Dannenberg, S. Dapprich, A.D. Daniels, Ö. Farkas, J.B. Foresman, J.V. Ortiz, J. Cioslowski, D.J. Fox, Gaussian 09, Revision D.01, Gaussian, Inc., Wallingford, CT, 2009.
[42] S.F. Boys, F. Bernardi, Mol. Phys. 19 (1970) 553.
[43] S. Simon, M. Duran, J.J. Dannenberg, J. Chem. Phys. 105 (1996) 11024.
[44] V. Barone, M. Cossi, J. Phys. Chem. A 102 (1998) 1995.
[45] M. Cossi, N. Rega, G. Scalmani, V. Barone, J. Comput. Chem. 24 (2003) 669.
[46] A.D. Becke, K.E. Edgecombe, J. Chem. Phys. 92 (1990) 5397.
[47] B. Silvi, A. Savin, Nature 371 (1994) 683.
[48] J.P. Piquemal, J. Pilmé, O. Parisel, H. Gérard, I. Fourré, J. Bergès, C. Gourlaouen, A. De La Lande, M.C. Van Severen, B. Silvi, Int. J. Quantum Chem. 108 (2008) 1951.
[49] E.R. Johnson, S. Keinan, P. Mori-Sanchez, J. Contreras-Garcia, A.J. Cohen, W. Yang, J. Am. Chem. Soc. 132 (2010) 6498.
[50] J. Contreras-Garcia, E.R. Johnson, S. Keinan, R. Chaudret, J.-P. Piquemal, D. Beratan, W. Yang, J. Chem. Theory Comput. 7 (2011) 625.